A Cryptic Vascular Endothelial Growth Factor T-Cell Epitope: Identification and Characterization by Mass Spectrometry and T-Cell Assays

Andreas O. Weinzierl,[1] Dominik Maurer,[1] Florian Altenberend,[1] Nicole Schneiderhan-Marra,[5] Karin Klingel,[3] Oliver Schoor,[1] Dorothee Wernet,[2] Thomas Joos,[5] Hans-Georg Rammensee,[1] and Stefan Stevanović[1,4]

[1]Department of Immunology, Institute for Cell Biology and [2]Institute of Clinical and Experimental Transfusion Medicine, University of Tübingen; [3]Department of Molecular Pathology, University Hospital Tübingen; [4]Proteome Centrum Tübingen, Tübingen, Germany and [5]NMI Natural and Medical Sciences Institute at the University of Tübingen, Reutlingen, Germany

Abstract

Vascular endothelial growth factor (VEGF) is involved in various physiologic processes, such as angiogenesis or wound healing, but is also crucial in pathologic events, such as tumor growth. Thus, clinical anti-VEGF treatments have been developed that could already show beneficial effects for cancer patients. In this article, we describe the first VEGF-derived $CD8^+$ T-cell epitope. The natural HLA ligand SRFGGAVVR was identified by differential mass spectrometry in two primary renal cell carcinomas (RCC) and was significantly overpresented on both tumor tissues. SRFGGAVVR is derived from a cryptic translated region of VEGF presumably by initiation of translation at the nonclassic start codon CUG^{499}. SRFGGAVVR-specific T cells were generated *in vitro* using peptide-loaded dendritic cells or artificial antigen-presenting cells. SRFGGAVVR-specific $CD8^+$ T cells, identified by HLA tetramer analysis after *in vitro* stimulation, were fully functional T effector cells, which were able to secrete IFN-γ on stimulation and killed tumor cells *in vitro*. Additionally, we have quantitatively analyzed VEGF mRNA and protein levels in RCC tumor and normal tissue samples by gene chip analysis, quantitative reverse transcription-PCR, *in situ* hybridization, and bead-based immunoassay. In the future, T cells directed against VEGF as a tumor-associated antigen may represent a possible way of combining peptide-based anti-VEGF immunotherapy with already existent anti-VEGF cancer therapies. [Cancer Res 2008; 68(7):2447–54]

Introduction

Vascular endothelial growth factor (VEGF), also known as vascular permeability factor, is a mitogen with high specificity for vascular endothelial cells. Its biological activities range from angiogenesis (1, 2), endothelial cell growth (3), and expression of antiapoptotic proteins, such as Bcl-2, in endothelial cells (4) to induction of vascular leakage (5) by activation of matrix metalloproteinase activity (6). Thus, VEGF is crucial in various physiologic and pathologic states, such as the formation of new blood vessels, wound healing, and tumor growth (see refs. 7, 8 for reviews).

The human *vegf* gene is organized in eight exons, which can be spliced alternatively into four major isoforms ($VEGF_{121}$, $VEGF_{165}$, $VEGF_{189}$, and $VEGF_{206}$; refs. 9, 10) and into two minor isoforms ($VEGF_{145}$ and $VEGF_{183}$; ref. 7). With increasing length of the VEGF isoform, the ability to bind to heparin also increases. $VEGF_{189}$ and $VEGF_{206}$ are highly basic and almost completely bound to the extracellular matrix. $VEGF_{121}$ is acidic, does not bind heparin, and thus is freely diffusible (11). $VEGF_{165}$ has intermediate properties regarding its secretion. As the mitogenic potency of VEGF decreases on loss of the heparin-binding region, $VEGF_{165}$ is twice as active as $VEGF_{121}$ (12) and thus has optimal bioavailability and biological activity (13–15). It has been shown that translation of the VEGF mRNA may be initiated not only at its presumed start codon at nucleotide 1039 (AUG^{1039}) but also at an in-frame CUG codon at nucleotide 499 (CUG^{499}). Use of CUG^{499} has been described for $VEGF_{121}$, $VEGF_{165}$, and $VEGF_{189}$. Although the exact extent of CUG^{499} usage differs between reports (16, 17), one can assume that transcription of $VEGF_{121}$ and $VEGF_{165}$ starts at CUG^{499} in >50% of the cases.

VEGF is in the spotlight of cancer therapy as its presence is crucial for neoangiogenesis. A tumor growing beyond a volume of 1 to 2 mm^3 requires its own blood vessels for a sufficient supply of nutrition and oxygen (18). Therefore, several strategies have been developed to hamper tumor vascularization by tackling VEGF signaling or levels of secreted VEGF. Several small molecules that interfere with VEGF signaling are being incorporated at present in clinical phase II trials. VEGF binds to two receptor tyrosine kinases (VEGFR-1 and VEGFR-2) present at the surface of most blood endothelial cells. VEGF binding leads to receptor dimerization, subsequent autophosphorylation, and activation of intracellular signaling cascades (19). VEGFR-1–expressing cells can be selectively killed by a recombinant fusion construct of $VEGF_{121}$ with the toxin gelonin (20). VEGFR-2, the major mediator of the mitogenic, angiogenic, and permeability enhancing effects of VEGF (7), can be blocked by several kinase inhibitors, such as sunitinib, sorafenib (21, 22), KRN951 (23), and AMG706 (24). To prevent VEGF from binding to its receptors, the monoclonal antibody bevacizumab has been developed. Bevacizumab is a humanized neutralizing VEGF antibody (25) that binds all biologically active forms of VEGF. In 2004, it was approved by the Food and Drug Administration for treatment of metastatic colorectal cancer. To summarize, various anti–VEGF-based cancer therapies have been developed, several of which have a substantial clinical effect.

Note: Supplementary data for this article are available at Cancer Research Online (http://cancerres.aacrjournals.org/).

A.O. Weinzierl and D. Maurer contributed equally to this work.

Requests for reprints: Stefan Stevanović, Department of Immunology, Institute for Cell Biology, University of Tübingen, Auf der Morgenstelle 15, 72076 Tübingen, Germany. Phone: 49-7071-29-87645; Fax: 49-7071-29-5653; E-mail: stefan.stevanovic@uni-tuebingen.de.

doi:10.1158/0008-5472.CAN-07-2540

Materials and Methods

Patient samples. No patient included in the experiments had received any anti–VEGF-based therapy. The following amounts of tissues were used for HLA peptide analysis: RCC099 (HLA-A*02, HLA-A*03, HLA-B*2705, and HLA-B*57): tumor tissue, 7.7 g; normal tissue, 12.4 g; RCC110 (HLA-A*02, HLA-A*68, HLA-B*18, and HLA-B*2705): tumor tissue, 7.0 g; normal tissue, 5.0 g.

Elution of HLA-presented peptides. HLA-presented peptides were obtained by immunoprecipitation of HLA molecules from solid tissues using an adapted protocol (26). One volume of 2× lysis buffer containing PBS, 0.6% CHAPS, and complete protease inhibitor (Roche Diagnostics) was added to shock frozen tissue samples. Subsequently, the samples were homogenized using a blender and afterwards by a potter. One volume of 1× lysis buffer was added and the lysate was stirred for 1 h at 4°C. After four times of 30 s of sonication, the sample was centrifuged at 3,000 × *g*, 4°C for 20 min, and afterwards at 150,000 × *g*, 4°C for 1 h, to remove cell debris. Finally, the sample was passed through a 0.2-μm filter (Sartorius). For immunoprecipitation, this lysate was applied for at least 12 h to a CNBr-activated Sepharose 4B column (40 mg Sepharose per mg tissue; GE Healthcare) to which the HLA-A–, HLA-B–, and HLA-C–specific antibody W6/32 had been coupled (1 mg antibody per mg tissue) as described by the manufacturer. After binding, the column was rinsed with 250 mL PBS and subsequently with 500 mL double-distilled water. For elution and dissociation of bound HLA-peptide complexes, the column was shaken at least four times in one bed volume of 0.1% trifluoroacetic acid (TFA) for 20 min at room temperature. The four TFA eluates were subsequently collected and combined. Finally, the HLA-presented peptides were isolated by ultrafiltration through a Centricon 10-kDa cutoff membrane (Millipore). For liquid chromatography-mass spectrometry (LC-MS) analysis, samples were freeze dried and resuspended in 0.1% formic acid or 0.1% TFA for modification.

Peptide modification and analysis. Modification of peptides (27) and peptide analysis (28) were carried out as described. For quantification, tumor and normal samples were mixed in a total peptide ratio of 1:1 and recorded in a single LC-MS experiment without fragmentation using a Q-TOF (Micromass). For sequence analysis, tumor and normal samples were analyzed separately in individual LC-MS/MS experiments. Interpretation of MS/MS fragmentation spectra was done as described elsewhere in detail (27).

Database searches. BLAST searches for SRFGGAVVR peptide sequence were performed using the PAM30 matrix (expect value < 1,000).[6] Protein versus protein searches (pBlast) were done in 245,584 sequences deposited in the SwissProt database; all species were included in the search. Translated protein versus nucleotide searches (tblastn) were done for all species using the National Center for Biotechnology Information (NCBI) nonredundant database (4,934,654 sequences), and expressed sequence tag sequences were excluded.

Histology and *in situ* hybridization. Cells expressing VEGF mRNA were detected by radioactive *in situ* hybridization (ISH) using single-stranded ^{35}S-labeled RNA probes, which were synthesized from human $VEGF_{121}$ cloned into pBluescript II SK (Stratagene). This pBSK-hVEGF121 plasmid was generously provided by Georg Breier (Institute of Pathology, Dresden, Germany). Paraffin tissue sections (5 μm) were treated as described previously (29).

Reverse transcription-PCR and quantitative reverse transcription-PCR. RNA from cells was isolated using Trizol reagent (Invitrogen) according to the manufacturer's recommendations. cDNA was synthesized from 1 μg total RNA. Real-time quantitative reverse transcription-PCR (qRT-PCR) using SYBR Green PCR Master Mix (Applied Biosystems) and expression analysis was performed as described (30). Primers were purchased from biomers.net: $VEGF_{121}$, 5′-AACATCACCATGCAGATTATGC-3′ (forward) and 5′-GGCTTGTCACATTTTTCTTGTC-3′ (reverse); $VEGF_{165}$, 5′-GTGAATGCAGACCAAAGAAAG-3′ (forward) and 5′-TTTTTGCAGGAA-CATTTACACG-3′ (reverse); and 18S, 5′-CGGCTACCACATCCAAGGAA-3′ (forward) and 5′-GCTGGAATTACCGCGGCT-3′ (reverse). For absolute quantification, standard curves of $VEGF_{121}$ and $VEGF_{165}$ were prepared using plasmids coding for the respective VEGF. Linear ranges of standard curves ranged from 10 fg to 10 ng of VEGF coding DNA. To calculate absolute VEGF copy numbers per cell, C_T values of the VEGF standard curve were allocated to C_T values of 18S RNA isolated from 2,000 JY-BLCL cells.

Gene expression analysis by high-density oligonucleotide microarrays. RNA isolation from tumor and autologous normal kidney specimens as well as gene expression analysis by Affymetrix Human Genome U133 Plus 2.0 oligonucleotide microarrays (Affymetrix) were performed as described (31). Microarray data are available from the Gene Expression Omnibus repository[7] with the accession number GSE8050.

VEGF protein quantification. Before the VEGF protein quantification, anti-VEGF beads were generated by covalent coupling of the anti-VEGF capture antibody to xMAP COOH Microspheres (Luminex). Tissue (40–80 mg) or 1×10^7 X63-B*2705 cells were pulverized and proteins were extracted with a 10-fold excess of solubilization buffer: 50 mmol/L Tris (pH 7.5), 400 mmol/L NaCl, 1 mmol/L $CaCl_2$, 1 mmol/L $MgCl_2$, 1% Triton X-100, and 1× complete protease inhibitor (Roche Diagnostics). After 1-h incubation on ice, cellular debris was removed. The total amount of solubilized protein was determined by Bradford assay. Subsequently, VEGF protein quantification was done as described (32) using a Luminex 100 IS (Luminex) and counting at least 100 beads.

Transfection of eukaryotic cells. The mouse myeloma cell line X63-B2705 [X63-Ag8.653 transfected with human HLA-B*2705 and human β2-microglobulin; generously provided by Elisabeth Weiss, Anthropologie und Humangenetik, Ludwig-Maximillians-Universität München, Munich, Germany (33)] was electroporated with various VEGF constructs. Transfected cells were maintained in RPMI 1640 (C.C.Pro) medium containing 10% FCS (Pan), 1 mg/mL G418S (Biochrom AG), and 0.4 mg/mL hygromycin (Roche Diagnostics).

***In vitro* stimulation of human $CD8^+$ T cells using dendritic cells.** T-cell culture medium consisted of RPMI 1640, 25 mmol/L HEPES, 2 mmol/L L-glutamine (all from Invitrogen), 10% heat-inactivated human AB serum (C.C.Pro), 50 units/mL penicillin, 50 μg/mL streptomycin, and 20 μg/mL gentamicin (all from Lonza). Isolation of peripheral blood mononuclear cells (PBMC) and dendritic cells (DC) was performed as described (34). DCs were pulsed for 2 h with 25 μg/mL of SRFGGAVVR peptide in T-cell culture medium and washed thrice with PBS before subsequent usage. *In vitro* stimulations were initiated in 24-well plates with 25×10^5 responder cells (autologous PBMCs, *in vitro* cultured for 1 wk) plus 5×10^5 DCs per well in 1.5 mL of T-cell culture medium. Cryopreserved, peptide-loaded, irradiated autologous PBMCs were used for restimulation after priming with DCs.

***In vitro* stimulation of human $CD8^+$ T cells using artificial antigen-presenting cells.** Untouched $CD8^+$ T cells were MACS enriched by negative depletion of PBMCs (Miltenyi Biotec). Stimulations were initiated in 96-well plates with 1×10^6 responder cells in 250 μL of T-cell culture medium complemented with 5 ng/mL human interleukin (IL)-12 (PromoKine) plus 2×10^5 microbeads coated with HLA-B*2705-SRFGGAVVR complexes, HLA-A*0201-NLVPMVATV complexes, plus anti-CD28 and anti-4-1BB antibodies as costimulatory signals (35). Subsequent stimulations with 80 units/mL human IL-2 (Chiron) were performed for 3 wk as described (34).

Tetramer staining. Tetramer analyses were performed with SRFGGAVVR-tetramer-APC, NLVPMVATV-tetramer-PE, and antibody CD8-PerCP clone SK1 (BD Biosciences). Cells were incubated with the antibody at 4°C for 20 min in the dark followed by 30-min incubation with fluorescent HLA tetramers in the dark at room temperature. After resuspending with PBS containing 1% paraformaldehyde, 0.5% bovine serum albumin, 2 mmol/L EDTA, and 0.02% NaN_3, cells were analyzed by flow cytometry on a four-color FACSCalibur cytometer (BD Biosciences).

Intracellular IFN-γ staining. Autologous PBMCs were pulsed with 10 μg/mL peptide and incubated with effector cells in a ratio of 1:1 for 6 h.

[6] http://www.ncbi.nlm.nih.gov/BLAST/

[7] http://www.ncbi.nih.gov/geo

GolgiStop (BD Biosciences) was added for the final 5 h of incubation. Cells were analyzed using a Cytofix/Cytoperm Plus kit (BD Biosciences), CD8-PerCP clone SK1 (BD Biosciences), and IFN-γ-PE (BD Biosciences). For negative controls, cells were incubated either with irrelevant peptide or without peptide, respectively. Stimulation with phorbol 12-myristate 13-acetate (PMA)/ionomycin was used as positive control. Cells were analyzed on a four-color FACSCalibur.

^{51}Cr release assay. SRFGGAVVR-PE tetramer-positive CD8$^+$ T cells were isolated using anti-PE MACS beads (Miltenyi Biotec). Cells were subsequently cultured in the presence of 5×10^5 cells/mL irradiated fresh allogenic PBMCs, 5×10^4 cells/mL irradiated LG2-EBV cells, 150 units/mL IL-2, and 0.5 μg/mL PHA-L (Roche Diagnostics). Target cells were labeled with 100 μCi Na_2 $^{51}CrO_4$ (Hartmann Analytic). Per well, 10,000 target cells were used at different E:T cell ratios in a standard 6-h ^{51}Cr release assay. Varying between different cell types, spontaneous releases ranged from 800 to 1,400 cpm, and maximal releases were in the range between 8,000 and 15,000 cpm.

Results and Discussion

A cryptic VEGF-derived HLA ligand identified by MS. Renal cell carcinoma of the clear cell type (RCC) is a frequent genitourinary tumor that is very resistant to standard therapy. To discover potential targets for T-cell–based tumor immunotherapy, we have analyzed the HLA ligandome of several RCCs and their autologous normal kidney tissue in detail (27, 31). Therefore, we isolated HLA-presented peptides from tumor and normal tissue, labeled the peptides with a stable isotope tag (28), and subjected them to LC coupled to an electrospray ionization mass spectrometer (ESI-LC-MS). All normal tissue–derived peptides were labeled NH_2 terminally with nicotinic acid (H_4-NIC); all peptides derived from tumor tissue were labeled in exactly the same manner but with a nicotinic acid bearing four deuterium atoms (D_4-NIC). The introduced isotope labels allowed, due to the isotopic mass shift, an accurate allocation of peptide signals to tumor or normal tissue after mixing of the two samples in a total peptide ratio of 1:1. Comparing the signal intensity of a heavy D_4-NIC peptide with its light H_4-NIC counterpart allowed peptide quantification between tumor and autologous normal tissue in one ESI-LC-MS experiment (27).

In such an analysis of RCC099, a very prominent tumor-derived peptide with *m/z* 529.3 attracted attention (Fig. 1*A*). After normalization to the average peptide presentation ratio (27), the quantitative analysis of this peptide showed a >6-fold overpresentation of the peptide in tumor (D_4-NIC) compared with normal tissue (H_4-NIC; Fig. 1*B, left*). In RCC110, the same peptide seemed >5-fold overpresented on tumor tissue (Fig. 1*B, right*). The corresponding peptide sequence (SRFGGAVVR) was identified by *de novo* sequencing using MS/MS (Fig. 1*C*). Furthermore, SRFGGAVVR fragmentation spectra from RCC samples were identical with fragmentation spectra of synthetic SRFGGAVVR (Fig. 1*C, bottom*). The peptide matched the HLA motif of HLA-B*2705 (score = 30)[8] for which both RCC099 and RCC110 were positive.

To identify the source protein from which the peptide SRFGGAVVR was derived, BLAST searches were performed against protein and translated nucleotide databases. Using the SwissProt protein database, no protein in any species was found containing the peptide SRFGGAVVR. However, searching in a translated nucleotide database, the SRFGGAVVR peptide was found in the "untranslated" region of VEGF in humans, chimpanzee, and rhesus monkey. SRFGGAVVR is in frame with the actual VEGF protein sequence and can be transcribed using the nonclassic CUG^{499} (16, 17) as start codon, thus being cryptic (Fig. 2). Furthermore, the COOH terminus of the peptide is predicted to be generated very efficiently by the proteasome (NetChop 3.0 software; score = 0.97).[9] Integrated bioinformatic approaches, assessing the whole antigen processing pathway, rank SRFGGAVVR at least in the top 2% of all HLA-B*27–presented peptides of VEGF (WAPP score MHC = 1.05, TAP = −48.58, proteasome = 3.31;[10] NetCTL, score = 1.68;[11] EpiJen, score = 1.498[12]).

Analysis of VEGF expression by ISH. To further characterize the cellular origin of VEGF leading to presentation of the SRFGGAVVR peptide in RCC tissue, ISH experiments with radioactively labeled VEGF RNA probes were performed in RCC tumors and autologous normal tissues. Lacking appropriate paraffin-embedded sample material for RCC099 and RCC110, this analysis was performed using three other clear cell RCCs (RCC135, RCC180, and RCC190) and their autologous normal tissues. In all analyzed samples, VEGF transcripts were only detected in tumor cells (Fig. 3*A–C*), thus being responsible for VEGF protein expression and subsequent presentation of the VEGF-derived peptide SRFGGAVVR. All autologous normal tissues (Fig. 3*D–F*), inflammatory cells (Fig. 3*D, if*), as well as endothelial cells of blood vessels within the tumor tissues (Fig. 3*A–C, bv*) were negative for VEGF mRNA.

Expression profile of VEGF variants in RCCs. Gene chip analysis of RCC099 and RCC110 showed a 2- to 4-fold overexpression of VEGF in tumor tissue (Table 1). However, the gene chip probe set detecting VEGF did not allow determination of the variant of VEGF expressed in tumor and normal tissue, respectively. Similarly, the ISH probe allowed no specific detection of any VEGF variant because it had a minimum of 90% sequence overlap with each VEGF variant.

A RT-PCR was therefore set up using primers covering the VEGF sequence from the classic ATG^{1039} start codon to the TGA^{1686} stop codon. $VEGF_{121}$ (459 nucleotides) and $VEGF_{165}$ (591 nucleotides) could subsequently be identified as the major transcript variants of VEGF in all analyzed samples (Fig. 4*A*). Moreover, minor amounts of $VEGF_{145}$ (531 nucleotides) and $VEGF_{189}$ (663 nucleotides) could also be detected.

In the same samples, VEGF amounts were analyzed by qRT-PCR in an absolute manner using defined amounts of reference plasmids coding for $VEGF_{121}$ and $VEGF_{165}$. Thus, $VEGF_{121}$-specific qRT-PCR primers were designed. In the case of $VEGF_{165}$, no specific qRT-PCR primer pair could be defined, which did not also recognize $VEGF_{189}$. Due to the very low amount of $VEGF_{189}$ expression (Fig. 4*A*), its contribution to $VEGF_{165}$-derived signals in qRT-PCR was put aside. $VEGF_{165}$ was expressed in RCC099 3-fold higher amounts than in $VEGF_{121}$ and in RCC110 7-fold (Fig. 4*B*), respectively. Comparing tumor and normal tissue, RCC099 showed only minor differences of mRNA expression levels for both VEGF variants. In contrast, RCC110 showed a minimum of 12-fold overexpression of VEGF in tumor tissue.

[8] http://www.syfpeithi.de

[9] http://www.cbs.dtu.dk/services/NetChop
[10] http://www-bs.informatik.uni-tuebingen.de/WAPP
[11] http://www.cbs.dtu.dk/services/NetCTL/
[12] http://www.jenner.ac.uk/EpiJen/

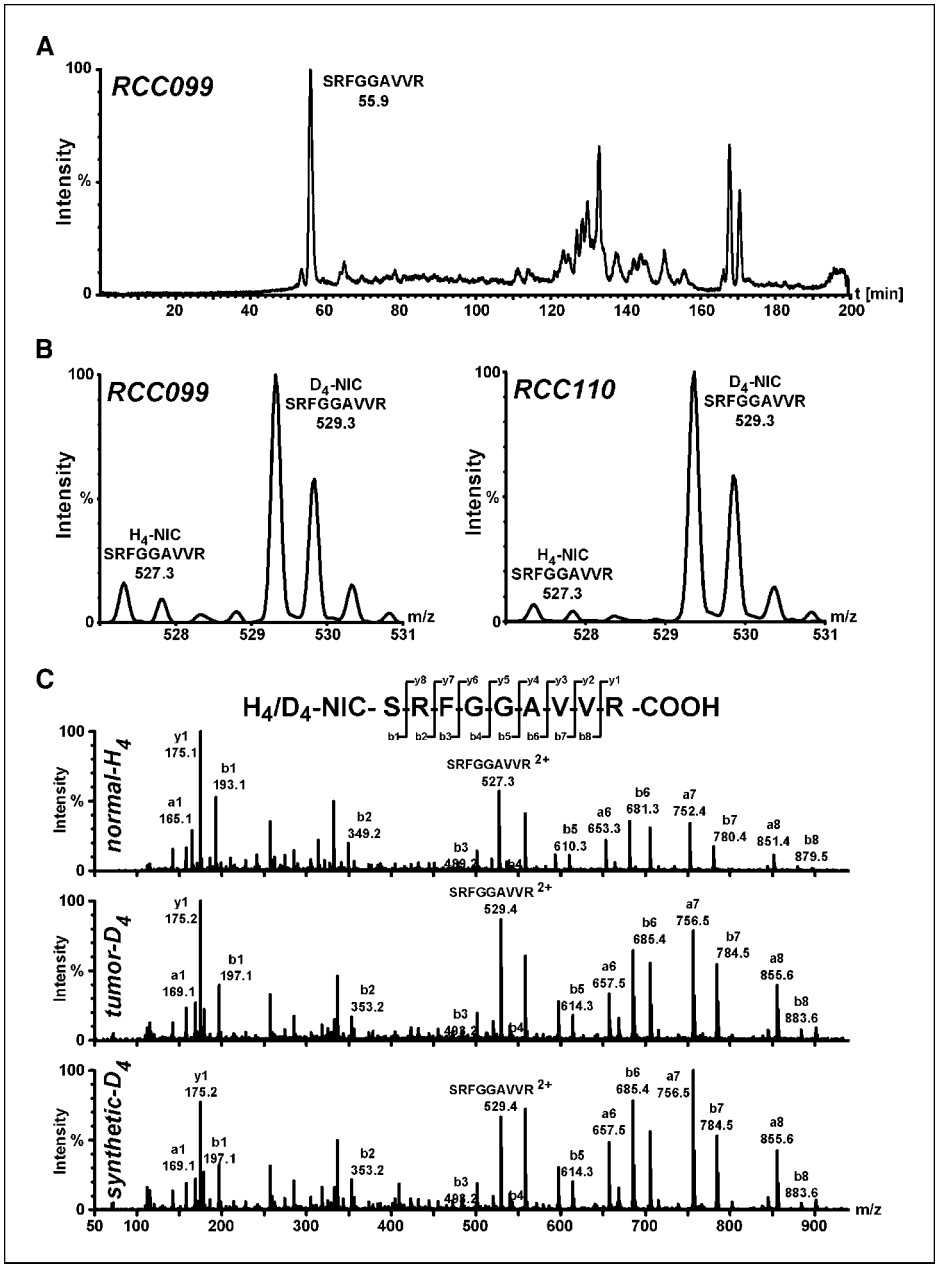

Figure 1. The SRFGGAVVR peptide is overpresented on HLA molecules of RCC099 and RCC110. HLA-presented peptides isolated from RCC099 and RCC110 were analyzed by MS. For analysis, samples were differentially labeled with an isotope tag. Tumor samples were modified with D_4-NIC, and normal tissue samples were modified with H_4-NIC. *A,* mass chromatogram of *m/z* 529.3 corresponding to D_4-NIC-SRFGGAVVR. *B,* ratio analysis of SRFGGAVVR presented on tumor (D_4-NIC-SRFGGAVVR; *m/z* 529.3) and normal tissue (H_4-NIC-SRFGGAVVR; *m/z* = 527.3). After normalization to the average presentation ratio, SRFGGAVVR seemed overpresented by 6.5-fold on RCC099 and 5.4-fold on RCC110. *C,* fragment spectra of differentially nicotinylated SRFGGAVVR derived from RCC099 tumor and normal tissue and fragment spectra of synthetic D_4-NIC-SRFGGAVVR.

Quantitative analysis of VEGF protein levels in RCCs. Correlation of mRNA with protein levels (36) and HLA ligand levels (27) is weak. Thus, protein levels of VEGF were assessed by a bead-based sandwich immunoassay (32) in RCC099 and RCC110 (Fig. 4*C, left*). Additionally, two other RCCs (RCC147 and RCC160), for which protein samples were available, were tested for VEGF protein expression. In all samples analyzed, VEGF protein expression was >4-fold higher in tumor compared with normal tissue. Protein ratios in both RCC099 and RCC110 were about four times higher as their corresponding mRNA ratios. This agrees with reports showing enhanced VEGF translation under hypoxic conditions (37).

Assessment of VEGF on various cellular levels. We analyzed VEGF on mRNA, protein, and HLA ligand levels (Table 1). Expression of VEGF mRNA in RCC tumor tissue has been described in several reports (38, 39). It is induced under hypoxic conditions mediated by the hypoxia-inducible factor (HIF)-1. In RCCs, in particular, it has been shown that inactivation of the von Hippel-Lindau tumor suppressor gene leads to excessive VEGF production (40) due to constitutive HIF-1 (41) and HIF-2 (42) activation. In 16 gene chip experiments (data not shown), we compared the expression of VEGF in primary RCC tissue and autologous normal kidney tissue and found VEGF overexpression (>3-fold) in ~70% of all cases. In 25% of all cases, overexpression was >9-fold. For RCC099 and RCC110, overexpression in tumor tissue was 2.0- and 4.7-fold, respectively. These gene chip data were confirmed by qRT-PCR. $VEGF_{121}$ and $VEGF_{165}$ were the predominant VEGF variants expressed in RCC, both being significantly overexpressed in tumor tissue. On the protein level, VEGF overexpression in tumor tissue was even more prominent. Here, differences ranged from 4- to 40-fold. Furthermore, the VEGF-derived peptide SRFGGAVVR was overpresented on HLA molecules in both tumor tissues. The extent

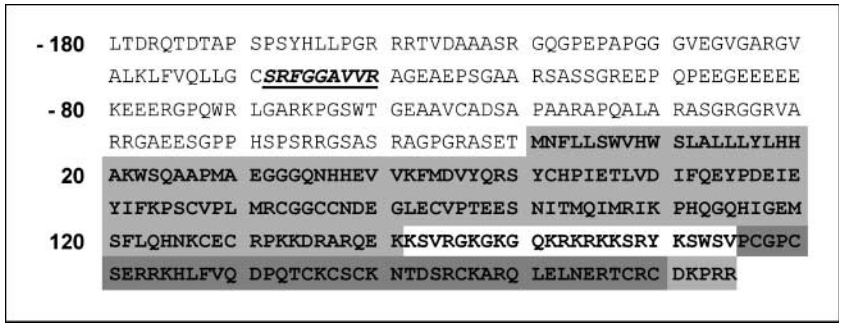

Figure 2. SRFGGAVVR is located in the untranslated region of VEGF. The translated protein sequence of VEGF mRNA (NCBI RefSeq Database ID NM_003376) starting at CUG[499] is shown. VEGF protein sequence as deposited in SwissProt (primary accession number P15692) is highlighted in bold. $VEGF_{121}$ is composed of amino acids shaded in light gray. The protein sequence of $VEGF_{165}$ additionally contains the amino acids shaded in dark gray. In-frame SRFGGAVVR is highlighted in bold italics and is underlined.

of HLA peptide overpresentation did not match its corresponding mRNA levels; this observation has been described previously for other gene products (27).

Generation of VEGF-expressing cell lines. For subsequent T-cell experiments, the mouse myeloma cell line X63-B*2705 (X63-Ag8 cells stably transfected with human HLA-B*2705 and β2-microglobulin) was used to circumvent contamination due to endogenous expression of human VEGF, which we could observe in human cell lines (see below). X63-B*2705 was stably transfected with two different VEGF constructs: VEGF-UTR165 was transfected with $VEGF_{165}$ containing the untranslated region and thus also containing the SRFGGAVVR peptide. VEGF-165 was transfected with $VEGF_{165}$ lacking the untranslated region and thus the SRFGGAVVR peptide. Surface expression of HLA-B*2705 was confirmed by fluorescence-activated cell sorting (FACS) analysis (data not shown), and VEGF protein expression was tested as described above (Fig. 4*D*).

Generation of VEGF-specific T cells. The VEGF-derived peptide SRFGGAVVR is presented by HLA-B*2705. To investigate whether the HLA-bound peptide can be recognized by functional cytotoxic T cells, $CD8^+$ T cells from healthy blood donors were stimulated *in vitro* for 4 weeks with DCs or artificial antigen-presenting cells (aAPC). All blood donors were HLA-A*0201 and HLA-B*2705 positive as well as seropositive for human cytomegalovirus (HCMV). For stimulation experiments, DCs were loaded with SRFGGAVVR peptide; aAPCs were loaded with costimulatory antibodies, HLA-B*2705-SRFGGAVVR complexes, and HLA-A*0201-NLVPMVATV complexes. The immunodominant HCMV-derived peptide NLVPMVATV served as positive control. After 4 weeks of stimulation, cells were stained with fluorescence-labeled B*2705-SRFGGAVVR or A*0201-NLVPMVATV tetramers and assayed in a FACS experiment. Both the HCMV-derived peptide and the VEGF-derived SRFGGAVVR were able to induce a specific T-cell population (Fig. 5*A*). In total, 16 HLA-B*27–positive healthy blood donors were tested for reactivity against the SRFGGAVVR peptide. In five donors, SRFGGAVVR tetramer-positive T cells could be expanded. Regarding these donors, ~5% of all stimulated wells (each containing 1×10^6 $CD8^+$ T cells) were positive in aAPC

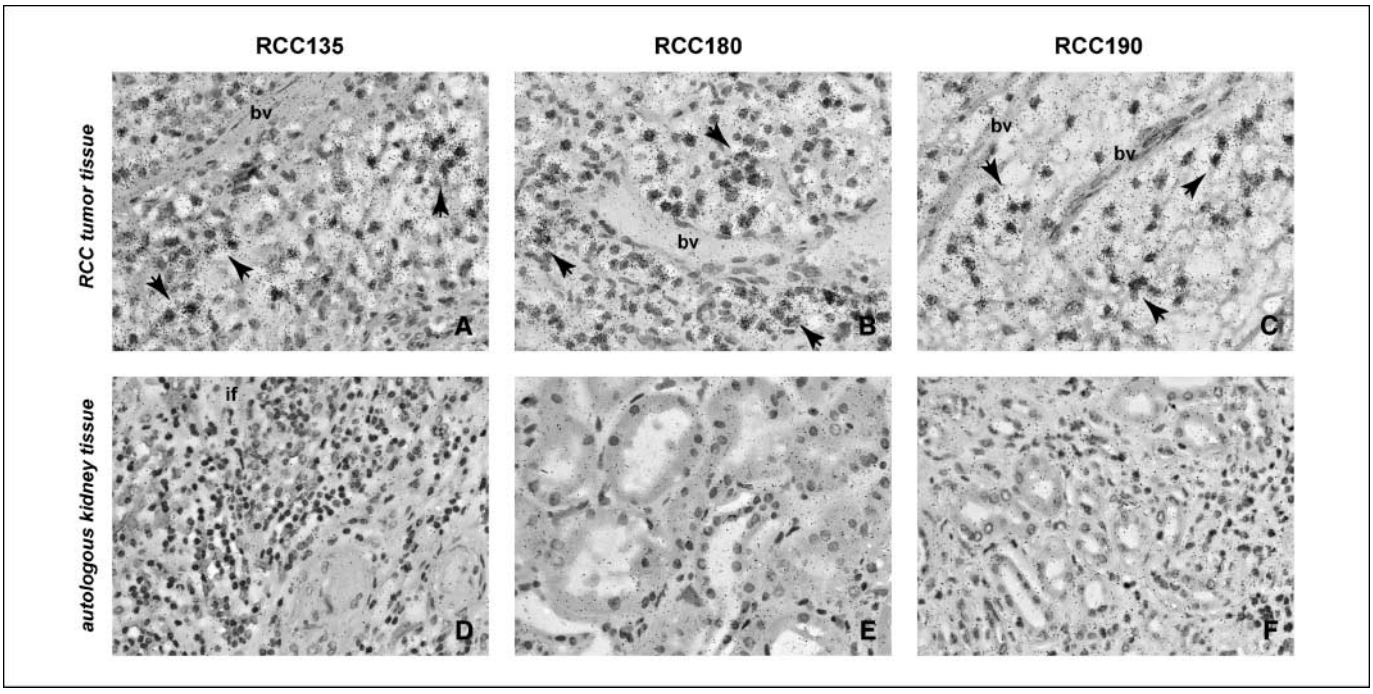

Figure 3. VEGF mRNA is expressed in tumor but not in autologous normal tissue as revealed by radioactive ISH. RCC135, RCC180, and RCC190 tumor (*A–C*) and autologous normal tissue (*D–F*) sections were stained with H&E. VEGF mRNA-expressing cells were detected by *in situ* hybridized, radioactively labeled $VEGF_{121}$ RNA. VEGF-positive cells are marked with arrows. No VEGF mRNA expression is detectable in normal tissue and renal tubuli of healthy kidneys. *bv,* blood vessels; *if,* infiltrating cells.

Table 1. VEGF ratios of tumor versus normal tissue are increased on various cellular levels

Sample	VEGF ratios (tumor vs normal tissue)			
	Gene chip	qRT-PCR	Protein	HLA ligand
RCC099	2.0	1.3	4.5	6.5
RCC110	4.7	12.9	42.1	5.4

NOTE: Protein, gene chip, and qRT-PCR refer to an average of $VEGF_{121}$ and $VEGF_{165}$ levels with potential minor contributions of $VEGF_{145}$ and $VEGF_{189}$; HLA-peptide ratio refers to presentation differences of the cryptic SRFGGAVVR peptide on HLA-B*2705.

stimulations. The frequency of SRFGGAVVR tetramer-positive cells ranged between 0.5% and 83.4%. Thus, the precursor frequency of SRFGGAVVR-specific T cells in healthy blood donors was estimated being in the magnitude of 0.5×10^{-7} to 1×10^{-7} according to the calculations by Carroll and Ashcroft (43). Due to this low frequency of SRFGGAVVR-specific T cells even after stimulation, positive reactions in the nine nonreactive blood donors may have been missed.

Functional analysis of VEGF-specific T cells. To assess the functionality of SRFGGAVVR-specific T cells, their ability to secrete cytokines and their cytolytic potential were analyzed. For these functional experiments, only DC stimulations were used because it has been reported that strong and rapid T-cell expansion using aAPCs bears the risk of inducing dysfunctional T cells (44). On coculture with autologous PBMCs loaded with SRFGGAVVR peptide, $CD8^+$ T cells were able to secrete IFN-γ. This confirmed that the effector T cells were functional and specific for VEGF (Fig. 5*B*). Furthermore, the cytolytic potential of these cells was analyzed in a chromium release assay. Therefore, *in vitro*–stimulated SRFGGAVVR-specific tetramer-positive T cells were MACS sorted and expanded. Autologous PBMCs loaded with an irrelevant peptide remained unlysed. Human C1R-B*2705 transfected with VEGF-UTR165 was lysed efficiently; however, the parental cell line C1R-B*2705 was lysed due to endogenous VEGF expression as well (data not shown). Mouse X63-B*2705 cells were recognized only after transfection with VEGF-UTR165 containing the cryptic SRFGGAVVR peptide sequence, whereas VEGF-165–transfected X63-B*2705 cells were not lysed, although VEGF-165 protein levels were 10-fold higher

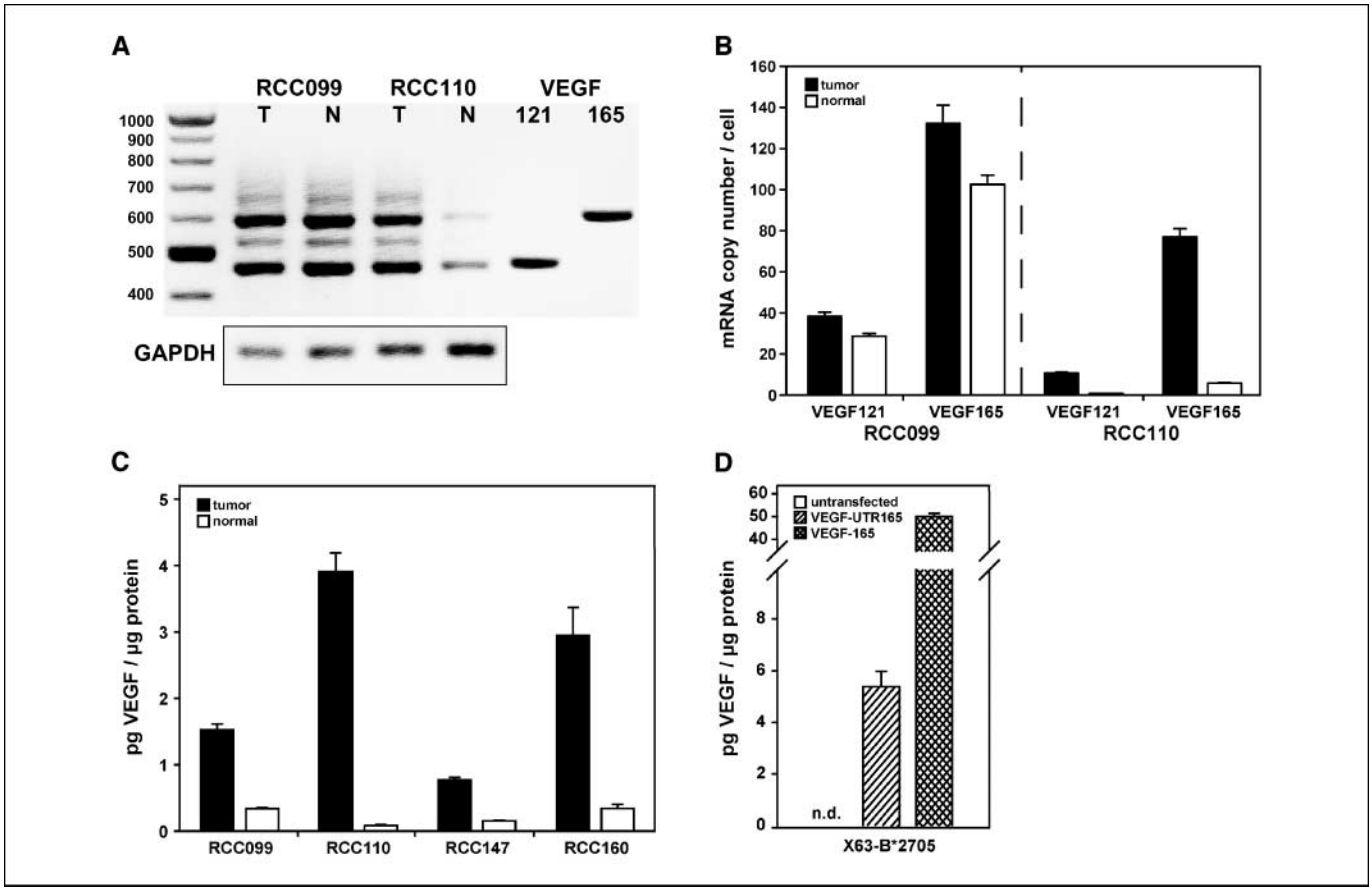

Figure 4. VEGF is overexpressed in RCC099 and RCC110 both on mRNA and protein levels. *A,* VEGF variants expressed in tumor (*T*) and normal (*N*) tissue were analyzed by RT-PCR by amplification of VEGF mRNA from nucleotides 1021 to 1689. $VEGF_{121}$ and $VEGF_{165}$ coding plasmids were used as reference samples. $VEGF_{145}$ and $VEGF_{189}$ are observable as faint bands in RCC099 and RCC110 samples. *GAPDH,* glyceraldehyde-3-phosphate dehydrogenase. *B,* absolute quantification of $VEGF_{121}$ and $VEGF_{165}$ by qRT-PCR. Plasmids coding for $VEGF_{121}$ and $VEGF_{165}$ were used as standards. Samples were normalized to 18S RNA isolated from 2,000 JY-BLCL cells. *C* and *D,* protein quantification of VEGF by bead-based sandwich immunoassay. *C,* four tumor and autologous tissues were analyzed. *D,* transfection efficiency of different VEGF constructs was determined in X63-B*2705 cells. In untransfected X63-B*2705 cells, VEGF was not detectable. *Columns,* mean; *bars,* SE.

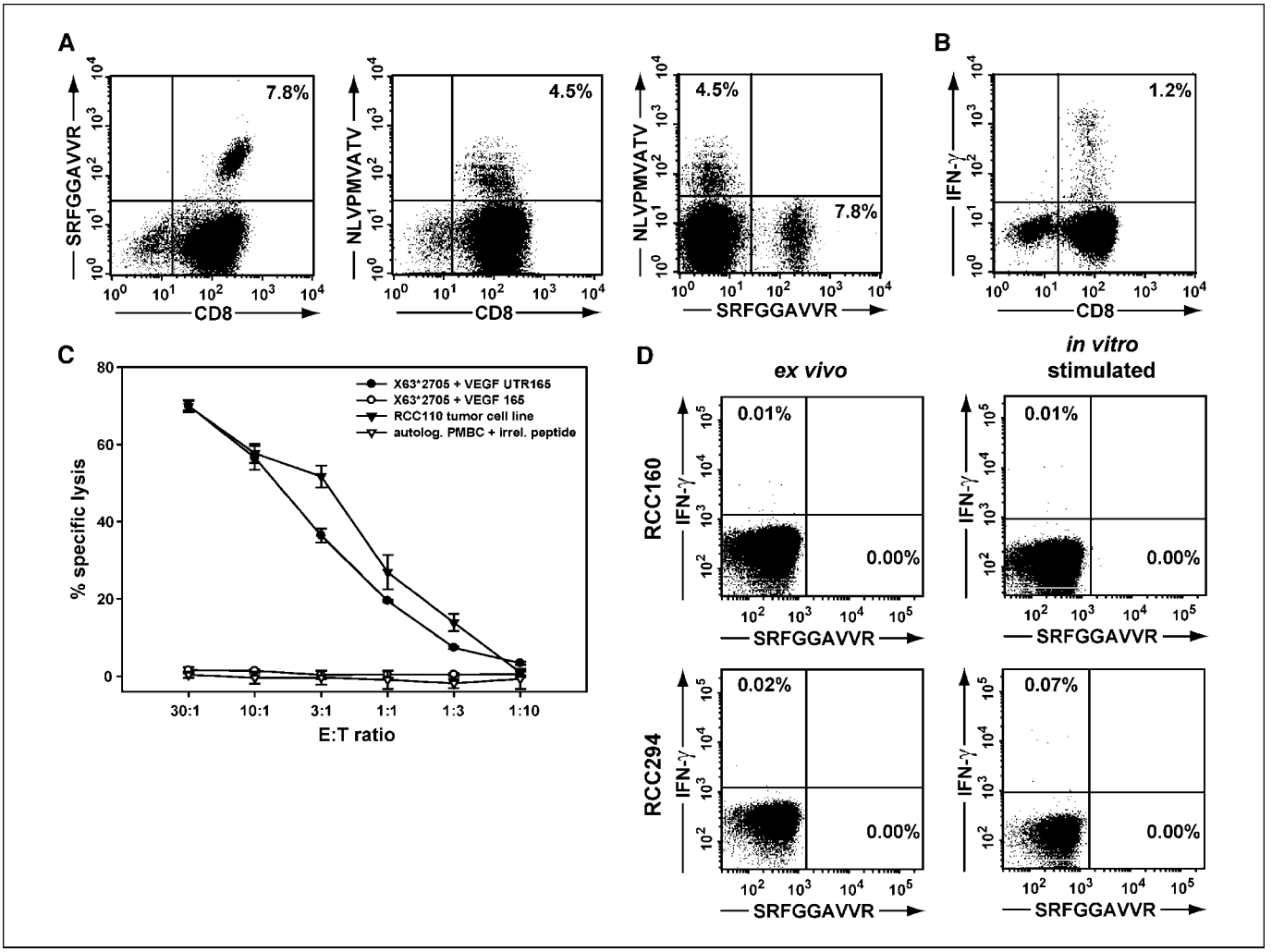

Figure 5. SRFGGAVVR-specific T cells are functional cytotoxic effector T cells. *A,* tetramer staining of CD8$^+$ T cells that were stimulated with aAPCs loaded with HLA-A*0201-NLVPMVATV (HCMV) and HLA-B*2705-SRFGGAVVR (VEGF) and with costimulating antibodies. The respective tetramer used for staining is indicated in each plot. Percentages are calculated from total CD8$^+$ cells. *B* and *C,* CD8$^+$ T cells, stimulated *in vitro* using DCs, were used for functional assays. Stimulated T cells were tested for IFN-γ secretion on coculture with autologous PBMCs loaded with SRFGGAVVR. *C,* ^{51}Cr cytotoxicity assay of SRFGGAVVR-stimulated CD8$^+$ T cells. Two X63-B*2705 transfectants, an RCC110 tumor cell line, as well as peptide-loaded autologous PBMCs were used as target cells. *Points,* mean; *bars,* SD. *D,* combined tetramer-IFN-γ analysis of PBMCs isolated from RCC160 and RCC294. Cells were stained *ex vivo* after 1 wk of *in vitro* stimulation with SRFGGAVVR peptide. Percentages are calculated from total CD8$^+$ cells, and irrelevant peptide stimulations resulted in identical percentages regarding the IFN-γ staining. Stimulation with PMA/ionomycin resulted in IFN-γ secretion of 70% to 90% of all CD8$^+$ T cells. Data are representative for PBMC samples from 10 other RCC patients.

than in VEGF-UTR165 cells (Fig. 4*D*). Finally, a cell line generated from RCC110 tumor tissue was specifically recognized by these T cells. Due to the fact that further maintenance of this SRFGGAVVR-specific T-cell line was not possible, determination of T-cell receptor avidity by peptide titration as well as testing of an extended RCC panel was not possible. Furthermore, we were not able to expand all SRFGGAVVR tetramer-positive T-cell clones to an extent that performance of ^{51}Cr release assays was possible.

Absence of VEGF-specific T cells in blood of RCC patients. Using PBMCs from healthy blood donors, SRFGGAVVR-specific T cells were inducible *in vitro*. To asses whether such SRFGGAVVR-specific T cells were induced *in vivo* in RCC patients, we analyzed PBMC samples of 12 HLA-B*27–positive RCC patients by tetramer analysis and by intracellular IFN-γ staining. In none of the samples, including RCC110, were tetramer-positive or IFN-γ–producing cells detectable, neither in an *ex vivo* analysis nor on 7 days of *in vitro* peptide stimulation (Fig. 5*D*). This suggests that SRFGGAVVR may not be spontaneously recognized by T cells from RCC patients, which may indicate a possibility for a therapeutic use of VEGF-specific T cells. However, it may also reflect a lower precursor frequency than in healthy blood donors or a peripheral tolerance against VEGF induced by the tumor, which would have to be broken for an immunotherapeutic approach using potent adjuvants.

Outlook. To predict possible organs in which a T-cell–based anti-VEGF therapy could have adverse effects, we analyzed VEGF mRNA expression in 32 different normal tissue specimens by gene chip experiments. Of all tissues analyzed, VEGF mRNA was only detectable in 13 tissues (see Supplementary Table S1). Only prostate tissue showed a >1.5-fold increase of VEGF expression compared with a commercially available standard kidney sample. In contrast, the average increase of VEGF in RCCs also compared with the standard kidney tissue was >5.5-fold.

However, the low amount of VEGF mRNA in the genitourethral tract, the intestine, and skeletal muscle suggests that a T-cell–based VEGF immunotherapy might lead to similar side effects as anti-VEGF antibodies, namely, hypertension, proteinuria, and bleeding or abnormalities in wound healing.

Acknowledgments

Received 7/5/2007; revised 12/4/2007; accepted 12/31/2007.

Grant support: Deutsche Forschungsgemeinschaft grants SFB-TR19 (A.O. Weinzierl, K. Klingel, and S. Stevanović) and SFB 685 (D. Maurer and S. Stevanović); Bundesministerium für Bildung und Forschung grant NGFN2 (O. Schoor); European Union, Cancer Immunotherapy, LSHC-CT-2006 518234 (H-G. Rammensee); and Jürgen Manchot Stiftung (A.O. Weinzierl).

The costs of publication of this article were defrayed in part by the payment of page charges. This article must therefore be hereby marked *advertisement* in accordance with 18 U.S.C. Section 1734 solely to indicate this fact.

We thank Lynne Yakes for critical reading of the manuscript, Tobias Krüger for establishing a cell line from RCC110 tumor tissue, and Jörg Hennenlotter and Arnulf Stenzl for providing RCC sample material.

References

1. Leung DW, Cachianes G, Kuang WJ, et al. Vascular endothelial growth factor is a secreted angiogenic mitogen. Science 1989;246:1306–9.
2. Plouet J, Schilling J, Gospodarowicz D. Isolation and characterization of a newly identified endothelial cell mitogen produced by AtT-20 cells. EMBO J 1989;8:3801–6.
3. Ferrara N, Davis-Smyth T. The biology of vascular endothelial growth factor. Endocr Rev 1997;18:4–25.
4. Gerber HP, Dixit V, Ferrara N. Vascular endothelial growth factor induces expression of the antiapoptotic proteins Bcl-2 and A1 in vascular endothelial cells. J Biol Chem 1998;273:13313–6.
5. Senger DR, Galli SJ, Dvorak AM, et al. Tumor cells secrete a vascular permeability factor that promotes accumulation of ascites fluid. Science 1983;219:983–5.
6. Wang FQ, So J, Reierstad S, et al. Vascular endothelial growth factor-regulated ovarian cancer invasion and migration involves expression and activation of matrix metalloproteinases. Int J Cancer 2006;118:879–88.
7. Ferrara N, Gerber HP, LeCouter J. The biology of VEGF and its receptors. Nat Med 2003;9:669–76.
8. Thornton AD, Ravn P, Winslet M, et al. Angiogenesis inhibition with bevacizumab and the surgical management of colorectal cancer. Br J Surg 2006;93:1456–63.
9. Houck KA, Ferrara N, Winer J, et al. The vascular endothelial growth factor family: identification of a fourth molecular species and characterization of alternative splicing of RNA. Mol Endocrinol 1991;5:1806–14.
10. Tischer E, Mitchell R, Hartman T, et al. The human gene for vascular endothelial growth factor. Multiple protein forms are encoded through alternative exon splicing. J Biol Chem 1991;266:11947–54.
11. Houck KA, Leung DW, Rowland AM, et al. Dual regulation of vascular endothelial growth factor bioavailability by genetic and proteolytic mechanisms. J Biol Chem 1992;267:26031–7.
12. Keyt BA, Berleau LT, Nguyen HV, et al. The carboxyl-terminal domain (111-165) of vascular endothelial growth factor is critical for its mitogenic potency. J Biol Chem 1996;271:7788–95.
13. Carmeliet P, Ng YS, Nuyens D, et al. Impaired myocardial angiogenesis and ischemic cardiomyopathy in mice lacking the vascular endothelial growth factor isoforms VEGF164 and VEGF188. Nat Med 1999;5:495–502.
14. Ruhrberg C, Gerhardt H, Golding M, et al. Spatially restricted patterning cues provided by heparin-binding VEGF-A control blood vessel branching morphogenesis. Genes Dev 2002;16:2684–98.
15. Stalmans I, Ng YS, Rohan R, et al. Arteriolar and venular patterning in retinas of mice selectively expressing VEGF isoforms. J Clin Invest 2002;109:327–36.
16. Bornes S, Boulard M, Hieblot C, et al. Control of the vascular endothelial growth factor internal ribosome entry site (IRES) activity and translation initiation by alternatively spliced coding sequences. J Biol Chem 2004;279:18717–26.
17. Tee MK, Jaffe RB. A precursor form of vascular endothelial growth factor arises by initiation from an upstream in-frame CUG codon. Biochem J 2001;359:219–26.
18. Folkman J. Tumor angiogenesis: therapeutic implications. N Engl J Med 1971;285:1182–6.
19. Matsumoto T, Mugishima H. Signal transduction via vascular endothelial growth factor (VEGF) receptors and their roles in atherogenesis. J Atheroscler Thromb 2006;13:130–5.
20. Mohamedali KA, Poblenz AT, Sikes CR, et al. Inhibition of prostate tumor growth and bone remodeling by the vascular targeting agent VEGF121/rGel. Cancer Res 2006;66:10919–28.
21. Nathan P, Chao D, Brock C, et al. The place of VEGF inhibition in the current management of renal cell carcinoma. Br J Cancer 2006;94:1217–20.
22. Schrader AJ, Varga Z, Pfoertner S, et al. Treatment targeted at vascular endothelial growth factor: a promising approach to managing metastatic kidney cancer. BJU Int 2006;97:461–5.
23. Nakamura K, Taguchi E, Miura T, et al. KRN951, a highly potent inhibitor of vascular endothelial growth factor receptor tyrosine kinases, has antitumor activities and affects functional vascular properties. Cancer Res 2006;66:9134–42.
24. Polverino A, Coxon A, Starnes C, et al. AMG 706, an oral, multikinase inhibitor that selectively targets vascular endothelial growth factor, platelet-derived growth factor, and kit receptors, potently inhibits angiogenesis and induces regression in tumor xenografts. Cancer Res 2006;66:8715–21.
25. Presta LG, Chen H, O'Connor SJ, et al. Humanization of an anti-vascular endothelial growth factor monoclonal antibody for the therapy of solid tumors and other disorders. Cancer Res 1997;57:4593–9.
26. Lemmel C, Weik S, Eberle U, et al. Differential quantitative analysis of MHC ligands by mass spectrometry using stable isotope labeling. Nat Biotechnol 2004;22:450–4.
27. Falk K, Rötzschke O, Stevanovic S, et al. Allele-specific motifs revealed by sequencing of self-peptides eluted from MHC molecules. Nature 1991;351:290–6.
28. Weinzierl AO, Lemmel C, Schoor O, et al. Distorted relation between mRNA copy number and corresponding major histocompatibility complex ligand density on the cell surface. Mol Cell Proteomics 2007;6:102–13.
29. Klingel K, Hohenadl C, Canu A, et al. Ongoing enterovirus-induced myocarditis is associated with persistent heart muscle infection: quantitative analysis of virus replication, tissue damage, and inflammation. Proc Natl Acad Sci U S A 1992;89:314–8.
30. Schoor O, Weinschenk T, Hennenlotter J, et al. Moderate degradation does not preclude microarray analysis of small amounts of RNA. Biotechniques 2003;35:1192–201.
31. Krüger T, Schoor O, Lemmel C, et al. Lessons to be learned from primary renal cell carcinomas: novel tumor antigens and HLA ligands for immunotherapy. Cancer Immunol Immunother 2005;54:826–36.
32. Schneiderhan-Marra N, Kirn A, Döttinger A, et al. Protein microarrays—a promising tool for cancer diagnosis. Cancer Genomics Proteomics 2005;2:37–42.
33. Ulbrecht M, Honka T, Person S, et al. The HLA-E gene encodes two differentially regulated transcripts and a cell surface protein. J Immunol 1992;149:2945–53.
34. Altman JD, Moss PA, Goulder PJ, et al. Phenotypic analysis of antigen-specific T lymphocytes. Science 1996;274:94–6.
35. Rudolf D, Silberzahn T, Walter S, et al. Potent costimulation of human CD8 T cells by anti-4-1BB and anti-CD28 on synthetic artificial antigen presenting cells. Cancer Immunol Immunother 2007;57:175–83.
36. Walter S, Herrgen L, Schoor O, et al. Cutting edge: predetermined avidity of human CD8 T cells expanded on calibrated MHC/anti-CD28-coated microspheres. J Immunol 2003;171:4974–8.
37. Gygi SP, Rochon Y, Franza BR, et al. Correlation between protein and mRNA abundance in yeast. Mol Cell Biol 1999;19:1720–30.
38. Stein I, Itin A, Einat P, et al. Translation of vascular endothelial growth factor mRNA by internal ribosome entry: implications for translation under hypoxia. Mol Cell Biol 1998;18:3112–9.
39. Jacobsen J, Grankvist K, Rasmuson T, et al. Expression of vascular endothelial growth factor protein in human renal cell carcinoma. BJU Int 2004;93:297–302.
40. Nicol D, Hii SI, Walsh M, et al. Vascular endothelial growth factor expression is increased in renal cell carcinoma. J Urol 1997;157:1482–6.
41. Siemeister G, Weindel K, Mohrs K, et al. Reversion of deregulated expression of vascular endothelial growth factor in human renal carcinoma cells by von Hippel-Lindau tumor suppressor protein. Cancer Res 1996;56:2299–301.
42. Maxwell PH, Wiesener MS, Chang GW, et al. The tumour suppressor protein VHL targets hypoxia-inducible factors for oxygen-dependent proteolysis. Nature 1999;399:271–5.
43. Carroll VA, Ashcroft M. Role of hypoxia-inducible factor (HIF)-1α versus HIF-2α in the regulation of HIF target genes in response to hypoxia, insulin-like growth factor-I, or loss of von Hippel-Lindau function: implications for targeting the HIF pathway. Cancer Res 2006;66:6264–70.
44. Montes M, Rufer N, Appay V, et al. Optimum *in vitro* expansion of human antigen-specific CD8 T cells for adoptive transfer therapy. Clin Exp Immunol 2005;142:292–302.